Contribution from the Institute for Protein Research, Osaka University, Suita, Osaka, 565, Japan, and the Department of Synthetic Chemistry, Faculty of Engineering, Kyoto University, Sakyo-ku, Kyoto, 606, Japan

Resonance Raman Spectra of Metallo-*trans*-octaethylchlorins and Their Meso-γ,δ-deuterated and ^{15}N-Substituted Derivatives

Y. OZAKI,[1a] T. KITAGAWA,*[1a] and H. OGOSHI[1b]

Received November 16, 1978

As models of the chromophore of chlorophyll and heme *d*, metallo-*trans*-octaethylchlorin [M(OEC), M = Cu^{2+} and Ni^{2+}], Fe^{3+}(OEC)L (L = F and Cl, high spin), Fe^{3+}(OEC)L_2 [L = imidazole (Im), low spin], and meso-γ,δ-deuterated and ^{15}N-isotope-substituted Cu(OEC) were investigated by resonance Raman spectroscopy. Upon ^{15}N substitution of four pyrrolic nitrogens of Cu(OEC), an isotopic frequency shift was observed for several Raman lines, which reasonably corresponded to the ^{15}N-sensitive Raman lines of chlorophyll *a* reported by Lutz et al. The vibrational displacements of the pyrrolic nitrogens were calculated from the observed frequency shifts. The frequencies of methine-bridge stretching vibrations were shifted by ca. 5 cm^{-1} upon meso-γ,δ-deuteration and found to be utilizable as a spin-state indicator of the iron ion of Fe(OEC) derivatives and likewise for iron octaethylporphyrin [Fe(OEP)] derivatives. The Fe–L stretching mode of Fe(OEC)L was observed at 608 cm^{-1} for L = F and at 361 cm^{-1} for L = Cl and the L–Fe–L symmetric stretching mode of Fe(OEC)L_2 was at 303 cm^{-1} for L = Im, in good agreement with the corresponding frequencies of Fe(OEP) derivatives. The Raman lines of M(OEC) were more intensified upon excitation at 568.2 nm than at shorter wavelengths presumably due to resonance with Q band near 600 nm. The intensity enhancement was pronounced for Raman lines around 1100–1300 cm^{-1} for M(OEC) derivatives in contrast with the case of M(OEP) derivatives.

Introduction

Extensive studies of the vibrational properties of metalloporphyrins have offered fundamental knowledge for analyzing the resonance Raman spectra of hemoproteins.[2] Detailed analysis of the resonance Raman spectra of (octaethylporphyrinato)nickel(II) [Ni(OEP)][3] and the subsequent normal-coordinate calculations[4] have established the assignments of the resonance Raman lines of metalloporphyrin and hemoproteins as well. However, no resonance Raman study has been reported for metallochlorins yet. Metallochlorins differ from metalloporphyrins merely about saturation of one $C_\beta C_\beta$ bond of a pyrrolic ring in the conjugated macrocycle, but the absorption spectra of metallochlorins are distinctly different from those of metalloporphyrins.[5]

The magnesium complex of chlorin constitutes the essential framework of the chromophore of chlorophyll. The resonance Raman spectra of chlorophyll were observed by Lutz et al.[6-9] On the other hand, the iron complex of chlorin is equivalent to heme d which is one of the prosthetic groups of nitrite reductase.[10] Therefore Raman spectroscopic investigation of metallochlorins is of biological importance in addition to physicochemical interest to elucidate the effects of saturation of one $C_\beta C_\beta$ bond of the porphyrin ring. Thus, in the present study, we synthesized metallo-*trans*-octaethylchlorin [M(OEC)] and their meso-γ,δ-deuterated [M(OEC-d_2)] and ^{15}N-substituted ones [M(OEC-$^{15}N_4$)] and report their resonance Raman spectra.

Experimental Section

M(OEC) and M(OEC-d_2) were prepared by reported methods.[11-13] Deuterium substitution only at the γ and δ positions was confirmed for free base chlorin by complete disappearance of the ^1H NMR peak at 8.86 ppm and the presence of a peak at 9.87 ppm. Copper was incorporated into the deuterated chlorin in C_6D_6 and CH_3OD under an argon atmosphere. Nevertheless the mass spectrum indicated presence (ca. 30%) of the monodeuterated Cu(OEC) in Cu(OEC-d_2). Cu(OEC-$^{15}N_4$) was derived from Fe^{3+}(OEP-$^{15}N_4$)Cl by the method described previously.[12] The ^{15}N substitution of pyrrolic nitrogens was confirmed to be more than 97% by infrared and mass spectra.

Raman spectra were excited by an Ar–Kr mixed gas laser (Spectra Physics, Model 164) and were recorded on a Jeol 400D or Jeol 02AS Raman spectrometer. Frequency calibration of the spectrometer was performed with indene (600–1700 cm^{-1})[14] and D_2 gas (100–650 cm^{-1})[15] for each excitation line. The estimated errors of frequencies and depolarization ratios were within ±1 cm^{-1} and 0.1, respectively. Upon the measurement of Raman spectra, 300 μL of an ca. 0.3 mM M(OEC) solution (CH_2Cl_2, CD_2Cl_2, or THF) was put in a cylindrical cell [CD_2Cl_2 was only for Cu(OEC-d_2)]. Visible absorption spectra were recorded with a Hitachi 124 spectrophotometer.

Results

The polarized resonance Raman spectra of Ni(OEC), Cu(OEC), Cu(OEC-d_2), and Cu(OEC-$^{15}N_4$) in CH_2Cl_2 (CD_2Cl_2) upon excitation at 488.0 nm are shown in Figure 1. Through all the Raman spectra presented, solid lines and broken lines denote the parallel and perpendicular polarization components, respectively. The structure of the MN_4 core is presumably planar for both Ni(OEC) and Cu(OEC), and accordingly their Raman spectra were alike, although Ni(OEC) gave appreciably higher frequencies in the region above 1450 cm^{-1}. The Raman line of Cu(OEC) at 1157 cm^{-1} was overlapped with that of solvent but its presence was confirmed in the THF solution.

Upon γ,δ-deuteration of Cu(OEC), the 1643 (p), 1584 (ap), 1506 cm^{-1} (p) lines showed clearly the frequency shift toward lower frequency by 5, 4, and 4 cm^{-1}, respectively, and new Raman lines appeared at 1527 (ap) and 1294 cm^{-1} (ap) (p, polarized; dp, depolarized; ap, anomalously polarized). The amounts of frequency shifts upon deuteration were smaller compared with those of metalloporphyrins [10, 23, and 7 cm^{-1} for the corresponding Raman lines of Ni(OEP)].[16] Upon the ^{15}N substitution, on the other hand, the isotopic frequency shifts occurred to Raman lines of Cu(OEC) at 1372 (p), 1362 (p), 1317 (ap), 1157 (dp), and 1129 cm^{-1} (ap), which were shifted by 6, 5, 5, 9, and 19 cm^{-1}, respectively.

Figure 2 illustrates the visible absorption spectra of Fe^{3+}(OEC)Cl (high spin, solid line) and [Fe^{3+}(OEC)$(Im)_2$]Cl in CH_2Cl_2 (low spin, broken line, Im = imidazole). Both compounds gave a strong absorption band near 600 nm with weak sidebands at shorter wavelengths. The wavelengths of excitation lines are designated by arrows on the abscissa.

The resonance Raman spectra of [Fe^{3+}(OEC)$(Im)_2$]Cl upon excitation at 568.2, 530.9, 514.5, and 488.0 nm are shown in Figure 3. Due to the weak power of excitation light, the apparent intensities of Raman lines for the 568.2-nm excitation looked weaker than those for the 488.0-nm excitation, but actually the intensity enhancement was largest for excitation at 568.2 nm. This could be most clearly demonstrated by plotting the relative intensities of Raman lines to the 1424-cm^{-1} line of solvent vs. the excitation wavelengths, although it is not shown. The intensity enhancement was more pronounced for the Raman lines below 1300 cm^{-1}. It is noted that the intensity of the Raman line at 1641 cm^{-1} decreased markedly

0020-1669/79/1318-1772$01.00/0

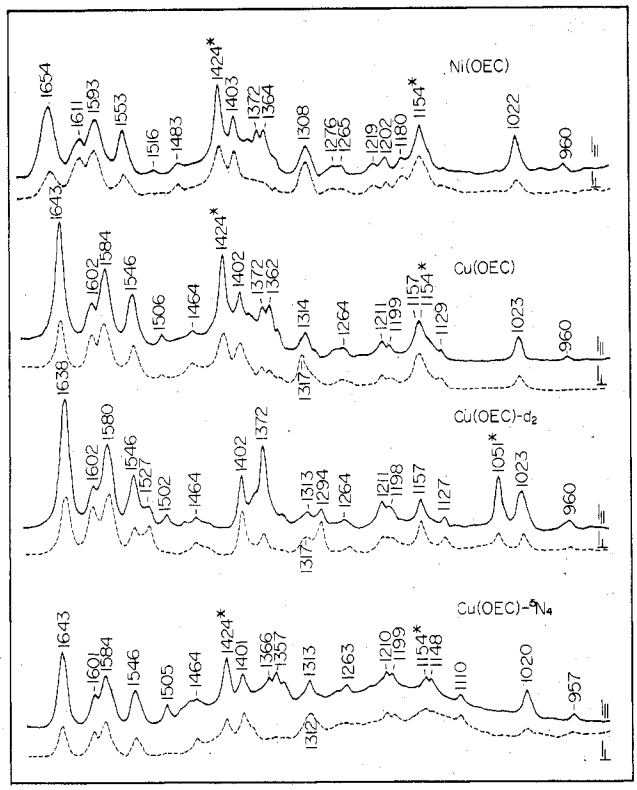

Figure 1. Polarized Raman spectra of Ni(OEC), Cu(OEC), Cu(OEC-d_2), and Cu(OEC-$^{15}N_4$) excited by the 488.0-nm line. Solid lines and broken lines denote the parallel and perpendicular polarization components, respectively. The Raman lines marked by an asterisk are due to solvent (1424 and 1154 cm^{-1} for CH_2Cl_2 and 1051 cm^{-1} for CD_2Cl_2). Only these spectra were measured with the use of a Jeol 400D Raman spectrometer equipped with a cooled HTV-R649 photomultiplier. Instrumental conditions are as follows: power, 200 mW; slit width, 3 cm^{-1}; sensitivity, 1000 counts/s; scan speed, 25 cm^{-1}/min; time constant, 3.2 s.

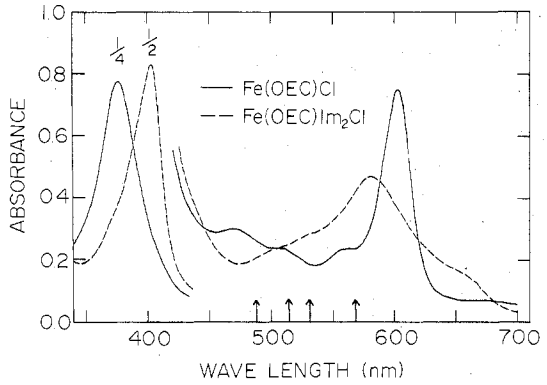

Figure 2. Visible absorption spectra of Fe^{3+}(OEC)Cl (solid line) and $[Fe^{3+}(OEC)(Im)_2]Cl$ in CH_2Cl_2 solution (broken line).

upon change of the excitation wavelength from 488.0 to 568.2 nm.

The resonance Raman spectra of Fe^{3+}(OEC)Cl in CH_2Cl_2 upon excitation at 568.2, 514.5, and 488.0 nm are shown in Figure 4. The Raman lines at 1130, 1210, 1233, and 1271 cm^{-1} were prominent upon excitation at 568.2 nm but were scarcely recognizable upon excitation at 488.0 nm, while the Raman line at 1629 cm^{-1} was weaker upon excitation at longer wavelengths. These trends were also observed for Ni(OEC) in contrast with the case of Ni(OEP) for which the Raman lines at 1138 and 1220 cm^{-1} were more enhanced upon excitation at shorter wavelengths while the highest frequency line at 1655 cm^{-1} was most intensified at Q band.[16] Therefore it would be characteristic of M(OEC) that vibrations around

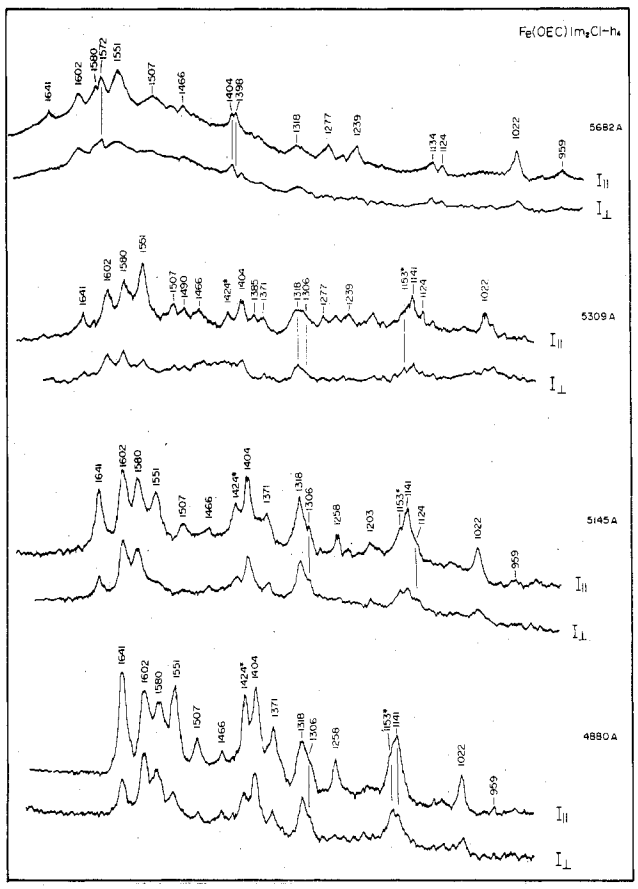

Figure 3. Raman spectra of $[Fe^{3+}(OEC)(Im)_2]Cl$ in CH_2Cl_2 excited at 568.2, 530.9, 514.5, and 488.0 nm. Instrumental conditions are as follows: power, 100–400 mW; slit width, 7 cm^{-1}; sensitivity, 1000 counts/s; scan speed, 9 cm^{-1}/min; time constant, 2.0 s; rate, 0.5 s.

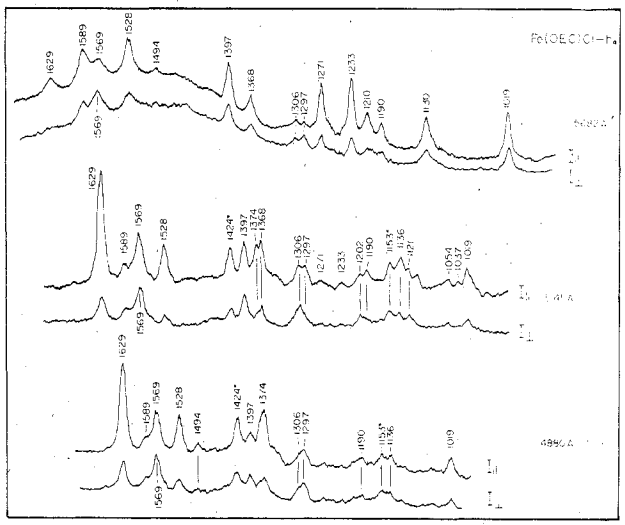

Figure 4. Raman spectra of Fe^{3+}(OEC)Cl in CH_2Cl_2 excited at 568.2, 514.5, and 488.0 nm. The instrumental conditions are the same as those for Figure 3.

1100–1300 cm^{-1} are more intensified in resonance with Q band compared with the vibrations above 1300 cm^{-1}.

The resonance Raman spectra of Fe^{3+}(OEC)F, Fe^{3+}(OEC)Cl, $[Fe^{3+}(OEC)(Im)_2]Cl$, and Ni(OEC) in THF in the lower frequency region are shown in Figure 5. The Raman spectrum of Fe^{3+}(OEC)F in the 900–1700-cm^{-1} region (not shown) was almost the same as that of Fe^{3+}(OEC)Cl. However, their difference was distinct for the Raman lines of Fe^{3+}(OEC)F at 608 cm^{-1} and of Fe^{3+}(OEC)Cl at 361 cm^{-1}; although there is a broad Raman line of the cell near 608 cm^{-1},

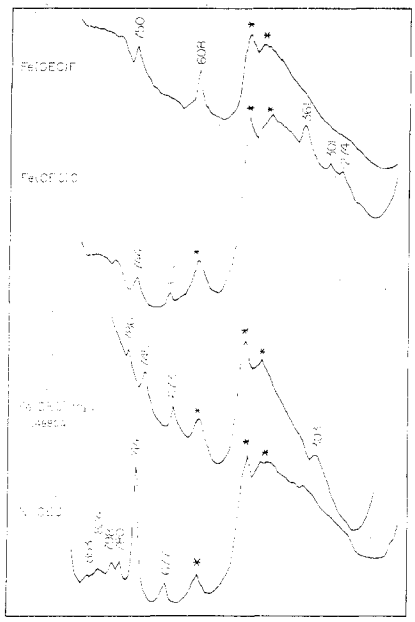

Figure 5. Raman spectra of Fe^{3+}(OEC)F, Fe^{3+}(OEC)Cl, Ni^{2+}(OEC), and $[Fe^{3+}(OEC)(Im)_2]Cl$ in THF in the frequency region of 850–100 cm^{-1}. The former three were excited at 514.5 nm but the last one was excited at 488.0 nm. The Raman lines marked by an asterisk are due to solvent or cell except for the 608-cm^{-1} line of Fe^{3+}(OEC)F (see text). Broad background below 500 cm^{-1} is due to cell. Instrumental conditions are same with those in Figure 3.

presence of a Raman line of Fe^{3+}(OEC)F at 608 cm^{-1} was inferred from its relative intensity. For Ni(OEC) and Cu(OEC), on the other hand, the corresponding Raman line was absent. The frequencies of these lines are in good agreement with those of Fe^{3+}(OEP)L (606 cm^{-1} for L = F and 364 cm^{-1} for L = Cl).[17] Accordingly, the 608- and 361-cm^{-1} lines were assigned, in the present study, to Fe–F and Fe–Cl stretching vibrations of Fe^{3+}(OEC)F and Fe^{3+}(OEC)Cl, respectively. This assignment is supported by the infrared frequencies of the Fe–L stretching mode of Fe(OEC)L in the solid state (589 cm^{-1} for L = F and 352 cm^{-1} for L = Cl).[11]

When two identical axial ligands are bound to the iron ion $[Fe(OEC)L_2]$, the L–Fe–L symmetric and antisymmetric stretching modes are fairly separated and the former would have lower frequency and stronger intensity. The Raman line of $[Fe^{3+}(OEC)(Im)_2]Cl$ at 303 cm^{-1} is presumably due to the Im–Fe–Im symmetric stretching mode. This frequency is close to the Im–Fe–Im symmetric stretching frequency of $[Fe^{3+}(OEP)(Im)_2]ClO_4$ (290 cm^{-1}).[17] The similarity of iron–axial ligand stretching frequencies between Fe(OEC) and Fe(OEP) in both high- and low-spin states may imply that the interaction between Fe and axial ligand is not affected significantly by saturation of one $C_\beta C_\beta$ bond and an accompanying change of electronic conjugation of the porphyrin ring.

Discussion

The molecular structure of M(OEC) is illustrated in Figure 6, where atomic and ring numberings and the Cartesian coordinate system are defined. The $C_\beta C_\beta$ bond of pyrrole IV of porphyrin is reduced in chlorin by two hydrogen atoms at trans positions and thus the symmetry of the π-electron framework is lowered to C_{2v} for M(OEC) compared with D_{4h} for Me(OEP). On meso-γ,δ-deuteration or ^{15}N substitution, the molecular symmetry of M(OEC) is retained. The symmetry correlation between D_{4h} and C_{2v} groups for the in-plane vibrations is represented in Table I. It is noted that the z axis for the D_{4h} group is perpendicular to the molecular plane in accord with the C_4 axis whereas the z axis for the C_{2v} group should coincide with the C_2 axis and therefore lies in the

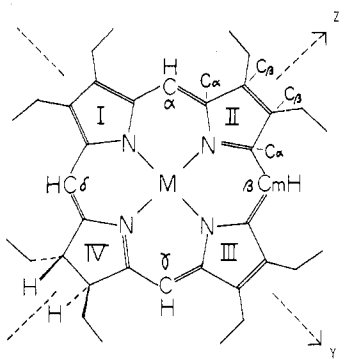

Figure 6. Chemical structure of metallo-*trans*-octaethylchlorin. The z and y axes are defined as shown in this figure and used for symmetry representation of M(OEC) of Table I. The structure of ethyl groups is arbitrary.

Table I. Symmetry Correlation between D_{4h} and C_{2v} Groups for the In-Plane Vibrations

D_{4h}	C_{2v}
$A_{1g}(p)^a$	
$B_{1g}(dp)$	$A_1(p)$
E_u	
$A_{2g}(ap)$	
$B_{2g}(dp)$	B_2(ap or dp)

[a] Polarization properties of Raman lines: p, polarized; dp, depolarized; ap, anomalously polarized.

molecular plane for M(OEC) (see Figure 6). The A_{1g} and B_{1g} vibrations of M(OEP) are symmetric to the C_2 axis, giving rise to the totally symmetric A_1 modes of M(OEC). The A_{2g} and B_{2g} vibrations of M(OEP) are antisymmetric to the C_2 axis and yield the B_2 modes of M(OEC). Degeneracy of the Raman-inactive E_u vibrations of M(OEP) is removed for M(OEC) and the split components are separated to the Raman-active A_1 and B_2 species of C_{2v}. Therefore, group-theoretically we may have more Raman lines for M(OEC) than for M(OEP).

The visible absorption spectra of M(OEC) were extensively discussed by Gurinovich and Sevchenko.[5] The Q band of M(OEP) is split into the $A_1(\mu_z)$ and $B_2(\mu_y)$ species for M(OEC) due to the lower symmetry. Accordingly the resonance enhancement of Raman intensity by the visible absorption bands is expected for the vibrations having the polarizability components of α_{zz} (A_1), α_{yy} (A_1), and α_{yz} (B_2). According to the tensor pattern for the two-photon process,[18] the A_1 and B_2 modes are expected to give the polarized and depolarized or anomalously polarized Raman lines, respectively. Since the vibrational modes of the resonance Raman-active species of Ni(OEP) have been interpreted recently,[4] the resonance Raman spectra of Cu(OEC) will be discussed in comparison with those of Ni(OEP) below.

There are eight $C_\alpha C_m$ stretching vibrations ($4A_1 + 4B_2$) for M(OEC) but four of them are expected to be extremely weak since they correspond to the E_u mode of the D_{4h} group. The Raman lines of Cu(OEC) at 1643 (p), 1584 (ap), and 1506 (p) cm^{-1} showed definite frequency shifts upon γ,δ-deuteration and therefore are considered to be associated with the $C_\alpha C_m$ stretching modes. These frequencies are close to those of Ni(OEP) at 1655 (ν_{10}, B_{1g}), 1603 (ν_{19}, A_{2g}), and 1519 cm^{-1} (ν_3, A_{1g}), which were assigned to the $C_\alpha C_m$ stretching modes previously.[4] It is presumed that the 1546-cm^{-1} line of Cu(OEC) may be a superposition of an anomalously polarized line and a polarized line, and only the anomalously polarized line may be shifted to 1527 cm^{-1} on meso-deuteration. Thus, the anomalously polarized line at 1546 cm^{-1} can be assigned to the other B_2 mode of the $C_\alpha C_m$ stretching vibrations of Cu(OEC), which would correspond to the unobserved B_{2g}

Table II. ^{15}N Isotopic Frequency Shifts and Vibrational Displacements of Pyrrole Nitrogen of Cu(OEC)

ν_a, cm^{-1}	polarizn	$\Delta\nu_a$, cm^{-1}	X_{Na}, Å
1372	p	6	0.011
1362	p	5	0.010
1317	ap	5	0.010
1157	dp	9	0.016
1129	ap	19	0.023

mode of the $C_\alpha C_m$ stretching vibrations of Ni(OEP).

Upon ^{15}N substitution the vibrations involving motion of nitrogen atoms are expected to show a frequency shift. The vibrational displacement of nitrogen atoms due to the ath vibration (X_{Na}) is estimated from the observed isotopic frequency shift ($\Delta\nu_a$) by eq 1.[19] Here ν_a^0 and ν_a are the frequencies for the normal and ^{15}N-substituted Cu(OEC), respectively, ^{14}m and ^{15}m are atomic masses of ^{14}N and ^{15}N, respectively, and Δm is their difference. The Raman lines of Cu(OEC) at 1372 (p), 1362 (p), 1317 (ap), 1157 (dp), and 1129 (ap) cm^{-1} clearly showed frequency shifts upon ^{15}N substitution. The observed shifts and the calculated root-mean-squared displacements of nitrogen atom are shown in Table II.

$$\langle X_{Na}^2\rangle_T = \frac{h(\nu_a^0 + \nu_a)}{8\pi^2\nu_a^3 c}\,\frac{\Delta\nu_a}{\Delta m}\,\frac{^{15}m}{^{14}m}\,\frac{[1+\exp(-h\nu_a/kT)]}{[1-\exp(-h\nu_a/kT)]} \quad (1)$$

For Ni(OEP), the Raman lines at 1383 (ν_4, A_{1g}), 1348 (ν_{12}, B_{1g}), 1159 (ν_{30}, B_{2g}) and 1121 cm^{-1} (ν_{22}, A_{2g}) showed the ^{15}N isotopic frequency shifts[3] and were assigned to the $C_\alpha N$ stretching modes.[4] Accordingly the 1372 (p), 1362 (p), 1157 (dp), and 1129 (ap) cm^{-1} lines of Cu(OEC) are presumably associated with the $C_\alpha N$ stretching modes and likewise with the ν_4, ν_{12}, ν_{30}, and ν_{22} modes of Ni(OEP), respectively. Their symmetry properties imply that the displacements of nitrogen atoms are toward the Cu ion for the former two modes whereas they are perpendicular to it for the latter two modes.

Lutz et al. reported the resonance Raman spectra of ^{15}N-substituted chlorophyll;[20] the Raman lines of chlorophyll a which showed larger isotopic frequency shifts are those of 1380 (7), 1350 (3–5), 1290 (8), 1225 (7), 1210 (8), 1147 (13), and 1115 cm^{-1} (11) in the 1650–1100-cm^{-1} region (number in parentheses indicates the isotopic frequency shift in wavenumber calculated from the reported values of $\Delta\nu/\nu$). On the basis of the ^{15}N sensitivity, the Raman lines of Cu(OEC) at 1372, 1362, 1317, 1157, and 1129 cm^{-1} may correspond to the Raman lines of chlorophyll a at 1380, 1350, 1290, 1147, and 1115 cm^{-1}, respectively. The slight differences of frequencies between Cu(OEC) and chlorophyll a are due to differences in the metal ion, the peripheral substituents, and the number of condenced rings.

The $C_\beta C_\beta$ stretching frequencies of Ni(OEP) are located at 1602 (ν_2, A_{1g}) and 1576 cm^{-1} (ν_{11}, B_{1g}).[4] These frequencies were insensitive to both meso-deuteration and ^{15}N substitution of Ni(OEP). The 1602- and 1546-cm^{-1} lines of Cu(OEC) were not shifted by both γ,δ-deuteration and ^{15}N substitution, and their frequencies were close to the frequencies of ν_2 and ν_{11} of Ni(OEP). Therefore, the two lines may be associated with the $C_\beta C_\beta$ stretching modes, although the observed polarization properties of Raman lines are inconsistent with the symmetry properties of these modes (A_1).

The frequencies of Raman lines of Fe(OEC) derivatives are compared with those of Fe(OEP) derivatives in Table III. The Raman lines corresponding to the spin-state indicator[21] of hemoproteins (bands I and III)[22] appeared at 1629 and 1494 cm^{-1} for Fe^{3+}(OEC)Cl (high spin) and at 1641 and 1507 cm^{-1} for [Fe^{3+}(OEC)(Im)$_2$]Cl (low spin), in good agreement with those at 1629 and 1493 cm^{-1} for Fe^{3+}(OEP)Cl (high spin) and at 1640 and 1506 cm^{-1} for [Fe^{3+}(OEP)(Im)$_2$]ClO_4 (low spin).[23] These lines are mainly due to the $C_\alpha C_m$ stretching modes.[5] This observation may indicate that the change of electronic state caused by saturation of one $C_\beta C_\beta$ bond perturbs little the bond strength of the $C_\alpha C_m$ bonds and that the change of spin state of the iron ion is transmitted to the $C_\alpha C_m$ bonds of the Fe(OEC) derivatives in a similar manner as is seen for the Fe(OEP) derivatives. Thus the frequencies of bands I and III can also be used as a spin-state indicator for proteins containing heme d, although no data are available at this moment.

Table III. Comparison of the Observed Frequencies (cm^{-1}) of Raman Lines of the Fe(OEC) and Fe(OEP) Derivatives

high spin		low spin	
Fe^{3+}(OEC)Cl	Fe^{3+}(OEP)Cl	[Fe^{3+}(OEC)-(Im)$_2$]Cl	[Fe^{3+}(OEP)-(Im)$_2$]ClO_4
1629 (p)	1629 (dp)	1641 (p)	1640 (dp)
1589 (ap)	1582 (dp)	1602 (ap)	1591 (dp)
1569 (ap)	1568 (ap)	1580 (ap)	1587 (ap)
1528 (p)	1545 (dp)	1551 (p)	1567 (dp)
1494 (p)	1493 (p)	1507 (p)	1506 (p)
1397 (dp)	1405 (dp)	1404 (dp)	1407 (dp)
1374 (p)	1374 (p)	1371 (p)	1374 (p)
1306 (ap)	1311 (ap)	1318 (ap)	1316 (ap)
1297 (ap)		1306 (ap)	
	1260 (p)	1258 (p)	1258 (p)
1153 (dp)	1153 (dp)	1153 (dp)	1154 (dp)
1136 (p)	1136 (p)	1141 (p)	1140 (p)
1019 (p)	1023 (p)	1022 (p)	1026 (p)

Intensity of some Raman lines of Fe^{3+}(OEC)Cl and [Fe^{3+}(OEC)(Im)$_2$]Cl was enhanced upon excitation at 568.2 nm but the corresponding lines of the Fe(OEP) derivatives were more intensified upon excitation at 488.0 nm.[16] Thus the wavelength giving a maximum in the excitation profile differed between the Fe(OEC) and Fe(OEP) derivatives. In addition some difference in the intensity-enhanced modes is noted; the vibrations above 1300 cm^{-1} were more enhanced at the Q band for Fe^{3+}(OEP)Cl than the lower frequency modes,[16] but the vibrations in the region of 1100–1300 cm^{-1} were intensified for Fe^{3+}(OEC)Cl. This feature was commonly observed for [Fe^{3+}(OEC)(Im)$_2$]Cl and Ni(OEC), too. On the other hand, a prominent difference in absorption spectra between Fe(OEC) and Fe(OEP) derivatives is seen for the relative intensity of the Soret and Q bands besides their band positions; the ratio of their absorbances, $\epsilon_Q/\epsilon_{Soret}$, is much larger for Fe(OEC) than for Fe(OEP) derivatives and the Q band is shifted to longer wavelength for Fe(OEC) derivatives. These may result in relatively strong enhancement of Raman intensity of Fe(OEC) derivatives upon excitation at 568.2 nm.

The resonance enhancement of Raman intensity generally occurs to the modes which experience the molecular geometry at an electronically excited state during the vibration[24] when they are totally symmetric modes. The polarized Raman lines of Fe^{3+}(OEC)Cl at 1019 cm^{-1} and of [Fe^{3+}(OEC)(Im)$_2$]Cl at 1022 cm^{-1} are deduced to involve a large contribution of the $C_\alpha C_m$ stretching mode as the corresponding lines of Fe(OEP) derivatives.[4] Therefore the intensity enhancement of these two lines upon excitation at 568.2 nm would imply appreciable stretch of the $C_\alpha C_\beta$ bonds upon electronic excitation at the Q band. On the other hand, for nontotally symmetric modes, vibronic coupling of two electronically excited states should be responsible for the intensity enhancement.[25] Gouterman[26] pointed out the intense 600-nm band of M(OEC) is assignable to the 0–0 transition of Q_y while the remaining weak bands around 500–600 nm are assignable to the 0–0 transition of Q_z and the 0–1 transitions of Q_y and Q_z. The fact that the intensity of methine bridge stretching Raman lines (1629 cm^{-1} (p) for Fe^{3+}(OEC)Cl and 1641 cm^{-1} (p) for [Fe^{3+}(OEC)(Im)$_2$]Cl) was decreased upon excitation at 568.2 nm and instead the modes around 1100–1300 cm^{-1}

were more intensified may implicate that such vibronic coupling occurs through the $C_\alpha C_\beta$ and $C_\alpha N$ bonds rather than the $C_\alpha C_m$ and $C_\beta C_\beta$ bonds, because the former contribute more to the modes around 1100–1300 cm^{-1}.[4] Alternatively negative interference of resonance effects of two different absorption bands[27] may have occurred to the methine bridge stretching modes upon excitation at 568.2 nm. For the determination of the alternatives, observation of detailed structure of excitation profile with dye laser is indispensable and such a study is under progress for Ni(OEC).

Acknowledgment. The authors wish to express their gratitude to Dr. Kenkichi Sonogashira, Osaka University, for the courtesy of measuring the mass spectra.

Registry No. Ni(OEC), 54676-28-7; Cu(OEC), 54676-27-6; Cu(OEC-d_2), 70101-72-3; Cu(OEC-$^{15}N_4$), 70116-74-4; Fe^{3+}(OEC)Cl, 54643-22-0; [Fe^{3+}(OEC)$(Im)_2$]Cl, 70096-17-2; Fe^{3+}(OEC)F, 54643-21-9.

References and Notes

(1) (a) Osaka University. (b) Kyoto University.
(2) (a) Kitagawa, T.; Ozaki, Y.; Kyogoku, Y. *Adv. Biophys.* **1978**, *11*, 153. (b) Spiro, T. G. *Biochim. Biophys. Acta* **1975**, *416*, 169 and references cited therein.
(3) Kitagawa, T.; Abe, M.; Ogoshi, H. *J. Chem. Phys.* **1978**, *69*, 4516.
(4) Abe, M.; Kitagawa, T.; Kyogoku, Y. *J. Chem. Phys.* **1978**, *69*, 4526.
(5) Gurinovich, G. P.; Sevchenko, A. N.; Solov'ev, K. N. "Spectroscopy of Chlorophyll and Related Compounds", Izdatel'stvo Nauka; Tekhnika: Minsk, 1968 (English translation; AEC-TR-7199).
(6) Lutz, M. *C. R. Hebd. Seances Acad. Sci., Ser. B* **1972**, *275*, 497.
(7) Lutz, M.; Breton, J. *Biochem. Biophys. Res. Commun.* **1973**, *35*, 413.
(8) Lutz, M. *J. Raman Spectrosc.* **1974**, 2, 497.
(9) Lutz, M.; Kleo, J.; Reiss-Husson, F. *Biochem. Biophys. Res. Commun.* **1976**, *69*, 711.
(10) Nagata, Y.; Yamanaka, T.; Okunuki, K. *Biochim. Biophys. Acta* **1970**, *221*, 668.
(11) Ogoshi, H.; Watanabe, E.; Yoshida, Z.; Kincaid, J.; Nakamoto, K. *J. Am. Chem. Soc.* **1975**, *95*, 2845.
(12) Ogoshi, H.; Watanabe, E.; Yoshida, Z.; Kincaid, J.; Nakamoto, K. *Inorg. Chem.* **1975**, *14*, 1344.
(13) Bonnett, R.; Gale, I. A. D.; Stephenson, G. F. *J. Chem. Soc., Ser. C* **1967**, 1168.
(14) Hendra, P. J.; Loader, E. J. *Chem. Ind. (London)* **1968**, 718.
(15) Stoicheff, B. P. *Can. J. Phys.* **1957**, *35*, 730.
(16) Kitagawa, T.; Ogoshi, H.; Watanabe, E.; Yoshida, Z. *J. Phys. Chem.* **1975**, *79*, 2629.
(17) Kitagawa, T.; Abe, M.; Kyogoku, Y.; Ogoshi, H.; Watanabe, E.; Yoshida, Z. *J. Phys. Chem.* **1976**, *80*, 1181.
(18) McClain, W. M. *J. Chem. Phys.* **1971**, *55*, 2789.
(19) Miyazawa, T. *J. Mol. Spectrosc.* **1964**, *13*, 321.
(20) Lutz, M.; Kleo, J.; Gilet, R.; Henry M.; Plus, R.; Leicknam, J. P. *Proc. Int. Conf. Stable Isot. Chem., Biol., Med., 2nd* **1975**, 462.
(21) Spiro, T. G.; Strekas, T. C. *J. Am. Chem. Soc.* **1974**, *96*, 338.
(22) Kitagawa, T.; Iizuka, T.; Saito, M.; Kyogoku, Y. *Chem. Lett.* **1975**, 849; *J. Am. Chem. Soc.* **1976**, *98*, 5169.
(23) Kitagawa, T.; Ogoshi, H.; Watanabe, E.; Yoshida, Z. *Chem. Phys. Lett.* **1975**, *30*, 451.
(24) Hirakawa, A.; Tsuboi, M. *Science* **1975**, *188*, 359.
(25) Tang, J.; Albrecht, A. C. In "Raman Spectroscopy"; Szymanski, H. A., Ed.; Plenum Press: New York, 1970; pp 33–68.
(26) Gouterman, M. *J. Mol. Spectrosc.* **1961**, *6*, 138.
(27) Stein, P.; Miskowski, V.; Woodruff, W. H.; Griffin, J. P.; Werner, K. G.; Gaber, B. P.; Spiro, T. G. *J. Chem. Phys.* **1976**, *64*, 2159.

Contribution from the Chemistry Departments, Hunter College, City University of New York, New York, New York 10021, and Purdue University, West Lafayette, Indiana 47907

X-ray Photoelectron Spectra of *N*-Methyltetraphenylporphyrins: Evidence for a Correlation of Binding Energies with Metal–Nitrogen Bond Distances

DAVID K. LAVALLEE,*[1a] JOHN BRACE,[1b] and NICHOLAS WINOGRAD[1b,c]

Received August 3, 1978

X-ray photoelectron spectroscopic data are reported for *N*-methyltetraphenylporphyrin, its dicationic salt, and a number of metal complexes, with special attention given to the N 1s binding energies. The free-base N 1s energies are 397.6 and 399.9 eV, with the N–CH_3 nitrogen atom being perturbed to essentially the same extent as the N–H nitrogen atom. The spectrum of the acid shows an increase in the relative area of the peak at 399.9 eV, indicating protonation of the nonmethylated nitrogen atoms. The N 1s energies for the metal complexes (398.3 and 400.4 eV for Mn(*N*-CH_3TPP)Cl, 398.2 and 400.2 eV for Fe(*N*-CH_3TPP)Cl, 398.4 and 400.2 eV for Co(*N*-CH_3TPP)Cl, and 398.5 and 400.0 eV for Zn(*N*-CH_3TPP)Cl, with the lower energies due to the nonmethylated nitrogen atoms in each case) correspond to changes in the size of the metal atom. The metal atom perturbs the nonmethylated nitrogen atoms to a greater extent than the methylated nitrogen atom. The difference in these energies correlates in a linear fashion with differences in the respective metal–nitrogen bond lengths determined crystallographically. In the case of greatest difference in binding energies, Mn(*N*-CH_3TPP)Cl, the XPS data indicate a relatively strong interaction with the methylated nitrogen atom while in the case of the greatest bond length difference, Zn(*N*-CH_3TPP)Cl, very little interaction is evident.

Introduction

X-ray photoelectron spectroscopy (XPS or ESCA) has been applied to a limited extent in the study of molecules of biological interest.[2,3] Two features of XPS data indicate that this method may be useful in discerning differences in chemical bonding that would be advantageous in the study of such molecules: the range of binding energies for core electrons of one element in a variety of chemical environments is well removed from the range of energies for other biologically important elements, and the energy maxima for one element in a variety of chemical environments appear to correlate well with calculated electron densities.[4] The utility of the XPS technique must be judged in light of its sensitivity to changes in bond parameters.

A system providing for such an investigation is a series of metal complexes of *N*-methylporphyrins, especially of *N*-methyltetraphenylporphyrin.[5–15] These complexes serve as models of possible intermediates in the porphyrin metalation mechanism and have been used to investigate spectral[6,13] and kinetic properties[5,10,14–19] of porphyrins with significantly nonplanar coordination sites. They have been quite thoroughly characterized and provide a means for systematic comparison with non-N-alkylated porphyrins. The chlorozinc(II), chloromanganese(II), chlorocobalt(II), and chloroiron(II) com-

0020-1669/79/1318-1776$01.00/0